Facile synthesis of free-standing CeO_2 nanorods for photoelectrochemical applications†

Xihong Lu,[a] Dezhou Zheng,[a] Peng Zhang,[a] Chaolun Liang,[b] Peng Liu[a] and Yexiang Tong*[a]

Received 12th June 2010, Accepted 26th August 2010
DOI: 10.1039/c0cc01854f

Free-standing CeO_2 nanorods with different morphology grew directly on Ti substrates *via* an electrochemical assembly process, and their absorption edges show a remarkable red-shift to the visible region. Moreover, photoelectrochemical cell (PEC) measurements demonstrate these CeO_2 nanorods exhibit a photovoltaic response under visible light illumination ($\lambda \geq 390$ nm).

Nanoarrays such as nanorod arrays (NRAs), nanotube arrays (NTAs), and nanowire arrays (NWAs) are of great interest owing to their unique properties and wide potential applications in future nanotechnology. They are expected to play important roles in sensors, catalysts, solar cells, electrochemistry, photoelectrochemistry, the lithium-ion battery, and so on.[1–3] In recent years, considerable efforts have been devoted to preparation of nanoarrays, and various nanoarrays have been fabricated by means of chemical vapor deposition (CVD), vapor–liquid–solid (VLS), sol–gel, laser ablation, hydrothermal synthesis, electrodeposition, *etc.*[4–6] Among these methods, electrodeposition with the assistance of templates has proved to be a convenient and versatile method for generating uniform and ordered nanoarrays.[7,8] However, it usually involves complicated procedures including preparation and elimination of the templates to obtain the pure products. Thus, the development of a template-free electrochemical method for creating nanoarrays is still an important challenge.

Over the past few years, considerable efforts have been focused on TiO_2, ZnO, SnO_2, NiO and other transition metal oxides for photovoltaic devices.[9–12] However, much less notice has been taken of the rare earth oxides as photovoltaic materials owing to their large optical energy band gaps. As a functional rare earth oxide with excellent physical and chemical properties, CeO_2 is extensively utilized in catalysts, fuel cells, UV blockers, ceramics, oxygen storage capacitors and sensors.[13,14] Organic dye-free solar cells based on hierarchical CeO_2 mesostructures were demonstrated as early as 2004, but subsequent literature is rather sparse.[15,16] The main difficulty for photovoltaic applications is its wide band gap of ~3.19 eV arising from O2p → Ce4f transition. It is known that the properties of nanomaterials depend strongly on the morphology and size. Recent reports have found that the one-dimensional (1D) ceria can improve the redox and transport properties compared with bulk materials. Theoretically speaking, the aligned 1D nanoarrays usually exhibit a higher surface area and superior transport properties than those of disordered one-dimensional nanostructures.[17] The preparation of CeO_2 nanorods, nanotubes, nanowires with template-free methods has been depicted, but the investigation on CeO_2 and other metal oxide nanoarrays with template-free methods has seldom been reported.[18,19]

In this study, we present a facile template-free electrochemical approach to the large-scale growth of aligned CeO_2 NRAs from aqueous solution. Three types of CeO_2 NRAs were successfully grown on Ti substrates based on a seed-assisted electrochemical growth mechanism, and the morphology of the CeO_2 NRAs can be readily modulated by adjusting the concentration of NH_4Cl. The absorption edges of these CeO_2 NRAs show a remarkable red-shift to the visible region. Moreover, they exhibit a photovoltaic response under visible light illumination ($\lambda \geq 390$ nm). This present work not only provides a new insight for large-scale, low-cost, controllable growth of well-aligned NRAs on conductive substrates, but also offers a new opportunity to build electronic and photoelectronic devices based on CeO_2 NRAs.

The electrodeposition of CeO_2 NRAs was carried out in solution of 10 mM $Ce(NO_3)_3$ + 50 mM NH_4Cl + 50 mM KCl with a current density of 0.5 mA cm^{-2} for 120 min at 70 °C, and the typical XRD pattern and SEM images are shown in Fig. 1. The peaks from the XRD pattern (Fig. 1a) reveal the product is a fluorite cubic structure of CeO_2 (JCPDF card: 65-2975) with lattice constants a = 0.5411 nm. The obtained products are pure CeO_2 because no other peaks are detected besides Ti peaks that come from the substrates. The low magnification SEM images in

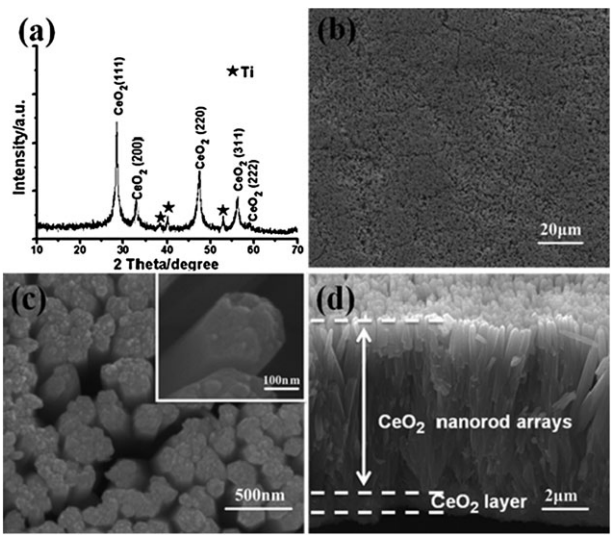

Fig. 1 (a) XRD pattern and (b–d) SEM images of the as-synthesized CeO_2 NRAs on Ti substrates.

[a] *MOE Key Laboratory of Bioinorganic and Synthetic Chemistry, School of Chemistry and Chemical Engineering, Institute of Optoelectronic and Functional Composite Materials, Sun Yat-sen University, Guangzhou 510275, China. E-mail: chedhx@mail.sysu.edu.cn; Fax: +86 20 84112245; Tel: +86 20 84110071*
[b] *Instrumental Analysis and Research Centre, Sun Yat-sen University, Guangzhou 510275, China*

† Electronic supplementary information (ESI) available: Detailed experimental section, potential–time curve, SEM images, XRD patterns, Raman and XPS spectra of CeO_2 nanorods. See DOI: 10.1039/c0cc01854f

Fig. 1b and c show the large scale of the well aligned CeO_2 rod arrays which successfully grew on Ti substrates. The high magnification SEM image (inset in Fig. 1c) indicates the diameter of a nanorod is about 200 nm and the top of the rod is coarse. The cross-sectional SEM image of the CeO_2 NRAs is given in Fig. 1d, showing that ordered nanorods of about 7.2 μm in length grew vertically from a CeO_2 layer. The thickness of the CeO_2 layer is around 0.87 μm, which is composed of CeO_2 particles (in Fig. S2a and b). In order to understand the growth mechanism of CeO_2 NRAs, the formation process of CeO_2 NRAs was studied by the potential–time curve and controlled experiments with different deposition time, as shown in Fig. S1–2 and discussed in the supporting information. It is believed that the preformed CeO_2 layer plays an important role as a seed layer for the growth of NRAs and the formation process of CeO_2 NRAs can be ascribed to a seed-assisted electrochemical growth mechanism.

The crystal structure of CeO_2 nanorods was investigated by TEM. A low-magnification TEM image of an individual nanorod is illustrated in Fig. 2a. The rod is a column-rodlike structure with a diameter of about 180 nm. Fig. 2c is the typical selected area electron diffraction (SAED) pattern of a nanorod. There are mainly two sets of electron diffraction patterns in this SAED pattern, which indicates the nanorod is highly crystalline with face-center cubic (fcc) structure and grows along the [110] direction. Fig. 2b shows the high-resolution TEM (HRTEM) image taken from the nanorod in Fig. 2a. The lattice spacing measured from the HRTEM image (insert in Fig. 2b) is about 0.31 nm, corresponding to the (111) plane of the fcc CeO_2. Fig. 2d displays a corresponding Fourier filtered (FFT) image of the rod (marked by a white rectangle in Fig. 2b), which exhibits some misfit dislocations. This indicates the presence of defects in the CeO_2 nanorod.

Fig. 3 shows the SEM images of two different CeO_2 NRAs, which are obtained *via* simply adjusting the NH_4Cl concentration. CeO_2 NRAs with the diameter of 400–500 nm and the length of about 2.7 μm were obtained for the 20 mM NH_4Cl, and these big rods were constructed by large numbers of wires with a small size, as shown in Fig. 3a–c. When the concentration of NH_4Cl was further increased to 100 mM, another different shape of CeO_2 arrays with a coarse surface was observed in Fig. 3c–f. The diameters and lengths of these nanorods are about 200–300 nm and 3.5 μm, respectively. Interestingly, this array was made up of nanorod bundles, and each bundle consists of an indefinite number of nanorods. Thus, the morphology of CeO_2 nanorods can be readily tuned by adjusting the concentration of NH_4Cl.

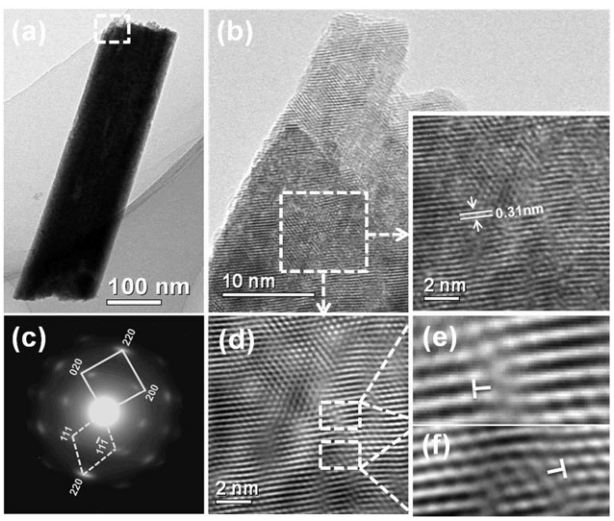

Fig. 2 (a) TEM, (b) HRTEM, and (c) SAED pattern of the CeO_2 NRAs on Ti substrates. (d) The corresponding Fourier filtered image of (b). (e–f) Enlarged images of the white rectangles marked in (d).

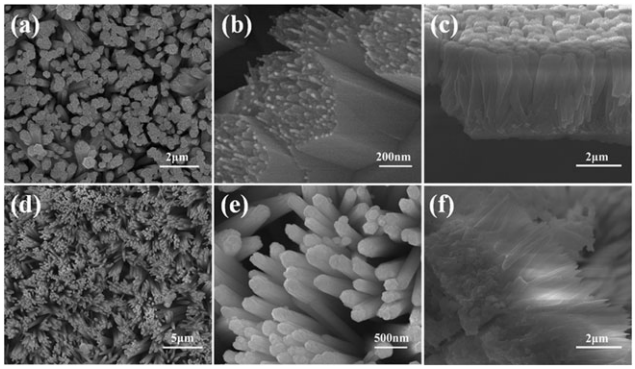

Fig. 3 SEM images of the CeO_2 NRAs prepared in (a–c) 20 mM and (d–f) 100 mM NH_4Cl.

Fig. 4a shows the UV-visible absorption spectra of these CeO_2 NRAs. The CeO_2 NRAs prepared in 20, 50 and 100 mM NH_4Cl were simply denoted as A-NRAs, B-NRAs and C-NRAs, respectively. Comparing to A-NRAs and C-NRAs, a clear red-shift (~10 nm) of the absorption band can be observed for B-NRAs. In addition, the adsorption bands of all samples have shifted toward the visible region. The calculated direct E_g for the three samples in Fig. 4b is about 2.86, 2.92, and 2.92 eV, respectively.[20] These values are comparatively smaller than the theoretical value of bulk CeO_2. We believed that the red-shift is mainly due to the surface defects, as demonstrated by HRTEM observations, Raman spectra, XPS results and discussed in the supporting information (Fig. S3–S5).

High aligned NRAs with narrow band gap are very desirable for the photovoltaic application since they can not only provide a high interfacial area but also provide a direct electron transport pathway.[21–23] In view of this, these three kinds of CeO_2 NRAs are expected to be used as photoelectrodes. And to the best of our knowledge, studies about the CeO_2 NRAs as photoelectrodes have never been reported so far. The photoelectrochemical properties of the three CeO_2 NRAs electrodes were characterized by measuring the photocurrent at zero bias under visible light illumination ($\lambda \geq 390$ nm). Fig. 5b shows the photocurrent response of the photoanodes prepared from the three kinds of CeO_2 NRAs. Surprisingly, all the CeO_2 NRAs exhibit an n-type semiconductor feature photovoltaic response under visible light

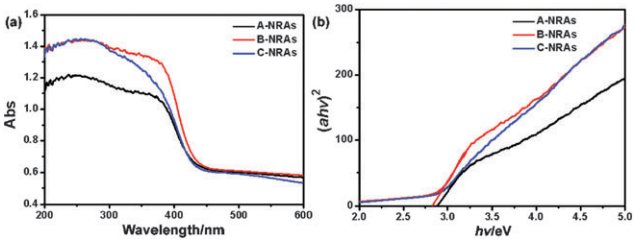

Fig. 4 (a) UV-visible absorption spectra and (b) $(\alpha h\nu)^2$ *vs.* $h\nu$ curves for these CeO_2 NRAs prepared in 20 mM NH_4Cl (A-NRAs), 50 mM NH_4Cl (B-NRAs), and 100 mM NH_4Cl (C-NRAs).

illumination. The B-NRAs electrode exhibited the best photoelectrochemical response: over 2 times higher than the A-NRAs and C-NRAs electrodes. The enhancement of photocurrent for B-NRAs can be attributed to the improvement of light-harvesting, as shown in Fig. 4a. In addition, all the samples are slow in generating photocurrent, which is caused by their intrinsic defects.

It is known that the photoelectrochemical activity is determined by both the capacity of light-harvesting and the separation of electron–hole pairs.[23,24] The electron–hole pairs are generated by absorbing the incident photons with energies larger than the E_g and they will recombine unless they are separated quickly. The schematic diagram of the CeO_2 NRAs photoelectrochemical cell is presented in Fig. 5a. In our case of CeO_2 NRAs, the electrons are first produced in the conduction band of CeO_2 nanorods under visible light illumination, and the corresponding holes are present in the valence band. Then the photogenerated electrons move through nanorods to the counter electrode for the reduction of water, while the holes move to the semiconductor/electrolyte interface for oxidation of methanol. The photoelectrochemical reactions are proposed as follows:[25]

$$h\nu \xrightarrow{CeO_2} h^+ + e^- \quad (1)$$

$$e^- + 2H^+ \rightarrow H_2 \quad (2)$$

$$h^+ + CH_3OH \rightarrow CH_3O^\bullet + H^+ \quad (3)$$

During this process, vertically-oriented CeO_2 NRAs provide a high interfacial area and superior electrical pathways for the transport of electrons, resulting in the reduction of electron–hole recombination and improvement of the photocurrent of these nanorod arrays. As for the slow photocurrent response for all the types of NRAs, it could be ascribed to the surface defects. As indicated by XPS and Raman spectra, the three CeO_2 samples possess large numbers of defects. These defects in CeO_2 NRAs might lead to the formation of a surface state energy band of oxygen and the oxygen adsorption, desorption and diffusion processes easily occur on the surface of the nanorods, which can greatly charge their properties such as optical and electrical properties.[26] When the incident light is larger than the E_g, the previous adsorbed oxygen on the surface of the nanorods will desorb and release free electrons, which cause the conductivity to increase. But then, it needs some time to achieve the steady state because the processes of absorption, desorption and diffusion of oxygen on the surface are very slow. Thus, the A-NRAs and B-NRAs show a slower photocurrent response than the C-NRAs, as shown in Fig. 5b.

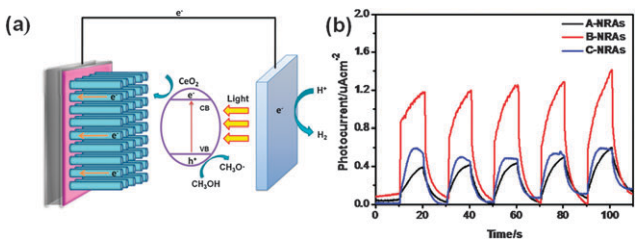

Fig. 5 (a) The schematic diagram of the CeO_2 NRAs photoelectrochemical cell and (b) photocurrent response of the photoanodes prepared from CeO_2 NRAs to light on–off under visible light illumination ($\lambda \geq 390$ nm).

In summary, three kinds of CeO_2 NRAs successfully grew on Ti substrates by an electrochemical assembly process without any templates or surfactants. The absorption edges of these NRAs all show a red-shift toward the visible region, and exhibit photovoltaic response under visible light illumination ($\lambda \geq 390$ nm). This study provides a new template-free electrochemical strategy for fabricating CeO_2 NRAs on conductive substrates as well as opportunities to build various photoelectrochemical devices based on CeO_2 NRAs.

This work was supported by the Natural Science Foundations of China (Grant No. 20873184, 90923008 and J20973205), the Natural Science Foundations of Guangdong Province (Grant No. 2008B010600040, 8151027501000095, and 9251027501000002), and the Yat-sen Innovative Talents Cultivation Program for Excellent Tutors.

Notes and references

1 Y. S. Zhao, P. Zhan, J. Kim, C. Sun and J. X. Huang, *ACS Nano*, 2010, **4**, 1630.
2 X. Y. Zhang, W. Lu, J. Y. Da, H. T. Wang, D. Y. Zhao and P. A. Webley, *Chem. Commun.*, 2009, 195.
3 X. J. Feng, K. Shankar, M. Paulose and C. A. Grimes, *Angew. Chem., Int. Ed.*, 2009, **48**, 8095.
4 S. H. Lee, G. H. Jo, W. J. Park, S. Lee, Y. S. Kim, B. K. Cho, T. Lee and W. B. Kim, *ACS Nano*, 2010, **4**, 1829.
5 J. Zhou, J. Liu, X. D. Wang, J. H. Song, R. Tummala, N. S. Xu and Z. L. Wang, *Small*, 2007, **3**, 622.
6 C. W. Xu, H. Wang, P. K. Shen and S. P. Jiang, *Adv. Mater.*, 2007, **19**, 4256.
7 M. V. Kamalakar and A. K. Raychaudhuri, *Adv. Mater.*, 2008, **20**, 149.
8 N. Shpaisman, U. Givan and F. Patolsky, *ACS Nano*, 2010, **4**, 1901.
9 Q. F. Zhang, C. S. Dandeneau, X. Y. Zhou and G. Z. Cao, *Adv. Mater.*, 2009, **21**, 4087.
10 P. Qin, M. Linder, T. Brinck, G. Boschloo, A. Hagfeldt and L. C. Sun, *Adv. Mater.*, 2009, **21**, 2993.
11 N. T. Hahn, H. Ye, D. V. Flaherty, A. J. Bard and C. B. Mullins, *ACS Nano*, 2010, **4**, 1977.
12 G. K. Mor, K. Shankar, M. Paulose, O. K. Varghese and C. A. Grimes, *Nano Lett.*, 2006, **6**, 215.
13 S. D. Park, J. M. Vohs and R. J. Gorte, *Nature*, 2000, **404**, 265.
14 C. W. Xu and P. K. Shen, *Chem. Commun.*, 2004, 2238.
15 A. Corma, P. Atienzar, H. Garcia and J.-Y. Chane-Ching, *Nat. Mater.*, 2004, **3**, 394.
16 M. Lira-Cantua and F. C. Krebs, *Sol. Energy Mater. Sol. Cells*, 2006, **90**, 2076.
17 L. Vayssieres, C. Sathe, S. M. Butorin, D. K. Shuh, J. Nordgren and J. H. Guo, *Adv. Mater.*, 2005, **17**, 2320.
18 C. S. Pan, D. S. Zhang, L. Y. Shi and J. H. Fang, *Eur. J. Inorg. Chem.*, 2008, 2429.
19 Y. G. Li, B. Tan and Y. Y. Wu, *J. Am. Chem. Soc.*, 2006, **128**, 14258.
20 D. Pradhan and K. T. Leung, *Langmuir*, 2008, **24**, 9707.
21 I. Gonzalez-Valls and M. Lira-Cantu, *Energy Environ. Sci.*, 2009, **2**, 19.
22 D. Kuang, J. Brillet, P. Chen, M. Takata, S. Uchida, H. Miura, K. Sumioka, S. M. Zakeeruddin and M. Grätzel, *ACS Nano*, 2008, **2**, 1113.
23 Y. Tak, S. J. Hong, J. S. Lee and K. J. Yong, *J. Mater. Chem.*, 2009, **19**, 5945.
24 J. Zhang, J. H. Bang, C. C. Tang and P. V. Kamat, *ACS Nano*, 2010, **4**, 387.
25 V. Korzhak, N. I. Ermokhina, A. L. Stroyuk, V. K. Bukhtiyarov, A. E. Raevskaya, V. I. Litvin, S. Y. Kuchmiy, V. G. Ilyin and P. A. Manorik, *J. Photochem. Photobiol., A*, 2008, **198**, 126.
26 Y. W. Zhang, R. Si, C. S. Liao, C. H. Yan, C. X. Xiao and Y. Kou, *J. Phys. Chem. B*, 2003, **107**, 10159.